Controlled photostability of luminescent nanocrystalline ZnO solution for selective detection of aldehydes†

Nikhil R. Jana, Hsiao-hua Yu, Emril Mohamed Ali, Yuangang Zheng and Jackie Y. Ying*

Received (in Cambridge, UK) 8th September 2006, Accepted 2nd January 2007
First published as an Advance Article on the web 30th January 2007
DOI: 10.1039/b613043g

Water-soluble, silane-functionalized ZnO nanocrystals were synthesized with improved colloidal stability, and their photostability was controlled for the selective detection of aldehydes.

Luminescent nanocrystals such as CdSe, CdTe, ZnSe and ZnO show great promise in molecular detection.[1] Their distinct optical properties,[2] such as high luminescence quantum yield, compositionally tunable emissions, and low susceptibility to photobleaching, offer distinct advantages over organic dyes. Of the II–VI nanocrystals, ZnO is of particular interest for various applications due to its low intrinsic toxicity as a "green" material in both manufacturing and applications.[3] The recent development of photoluminescent ZnO-based nanocrystals that demonstrate improved quantum yields[4] prompted us to apply them as molecular sensors for biological and chemical detection. Even though the photostability of a luminescent nanocrystal is very sensitive to its surface structure,[5] to our knowledge, the control over photostability has never been strategically and rationally employed in sensor applications. Herein we report the preparation of stable ZnO colloidal solutions through the surface silane modification of ZnO nanocrystals, and the selective detection of functional molecules by controlling the photostability of the nanocrystals' protective layer. Aldehyde functional groups are commonly present in important biomolecules and biointermediates. In this report, we also desribe a method that selectively recognizes the molecules bearing aldehyde groups through imine formation with our amino-functionalized ZnO nanocrystals (Scheme 1).

Silanization has been widely applied to provide colloids with stability and functionalized surfaces.[6] We synthesized the ZnO nanocrystals from a solution of zinc acetate and oleic acid in ethanol under reflux.[7] The reaction mixture was stirred and then quenched rapidly after mixing with boiling ethanolic tetramethylammonium hydroxide (TMAH) solution. After the solids were centrifuged, collected, and dispersed in toluene, the ZnO nanocrystals underwent two-stage silanization for surface modification. Trialkoxysilanes or trihydroxysilanes were initially added to the solution in the presence of exactly one equivalent of TMAH. Excess TMAH was then added to initiate the crosslinking. Utilizing this method, the formation of homocoupling siloxanes could be limited. This also ensured that the ZnO nanocrystals were surface-modified with silanes, and not trapped within siloxane clusters. After washing and drying, the ZnO nanocrystals were redissolved in water to prevent coagulation. Generally, stock solution of 3 mg mL^{-1} was prepared as it provided for optimal stability. Its luminescence intensity and emission peak remained unchanged for more than two weeks when the solution was stored at 4 °C in the dark.

Fig. 1(a) shows that the ZnO nanoparticles were crystalline and non-agglomerated. The silane coating was not observed in the high-resolution transmission electron microscopy (HRTEM) image, indicating that the surface coating was very thin. The ZnO nanocrystals showed a broad absorption that dropped at 350 nm in the ultraviolet region, and an emission peak at 545 nm (Fig. 1(b)). The luminescence of ZnO nanocrystals was due to surface trap effect,[8] thus, a broad emission peak of 120 nm bandwidth was obtained. Quantum yields of the ZnO nanocrystals were consistently measured at 16–20% with fluorescein as a standard. These values were higher than those reported in the literature for conventional ZnO nanocrystals.[9] X-ray diffraction (XRD) pattern of our ZnO nanocrystals[10] matched with the as-synthesized ZnO nanocrystals reported in the literature.[4a] TEM and XRD peak broadening analyses both indicated the ZnO nanocrystals to be ~5 nm. This two-stage silanization has successfully introduced a variety of functional groups onto the ZnO nanocrystals, including primary amine, tertiary amine, and phosphonates. These charged surface functional groups resulted in increased water solubility. The surface functional groups were characterized by nuclear magnetic resonance (NMR) spectra. In proton NMR spectra, a pair of signals at ~1.7 and 0.7 ppm with equal intensity clearly identified the first two Si-adjacent CH_2

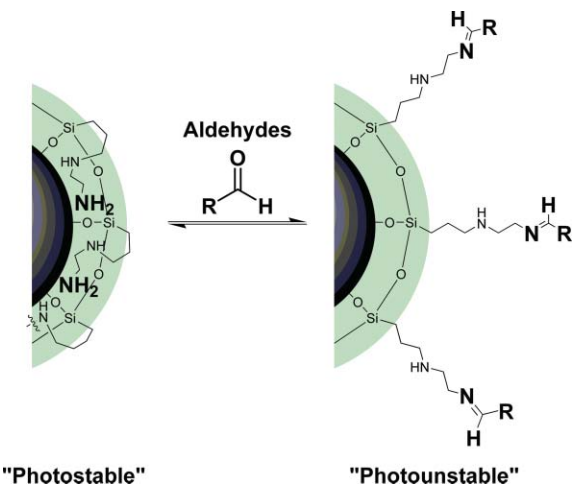

Scheme 1 Controlled photostability by interaction between NH_2–ZnO nanocrystals and aldehydes.

Institute of Bioengineering and Nanotechnology, 31 Bioplois Way, The Nanos, Singapore 138669. E-mail: jyying@ibn.a-star.edu.sg; Fax: +65-6478-9020

† Electronic supplementary information (ESI) available: Detailed synthetic procedure, XRD pattern, NMR spectra, and titration of the surface amino groups. See DOI: 10.1039/b613043g

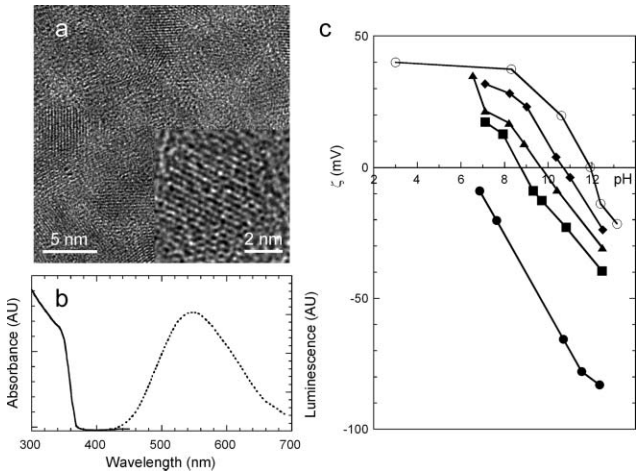

Fig. 1 (a) HRTEM micrographs of the silanized ZnO nanocrystals. (b) Absorption (—) and emission (···) spectra of the aminoethylamino-functionalized ZnO nanocrystals. (c) Plot of the pH dependence of the surface charge of the ZnO nanoparticles silanized using a mixture of AEAPS and phosphonate silane containing (●) 0, (■) 25, (▲) 50, (♦) 75 and (○) 100 mol% of AEAPS.

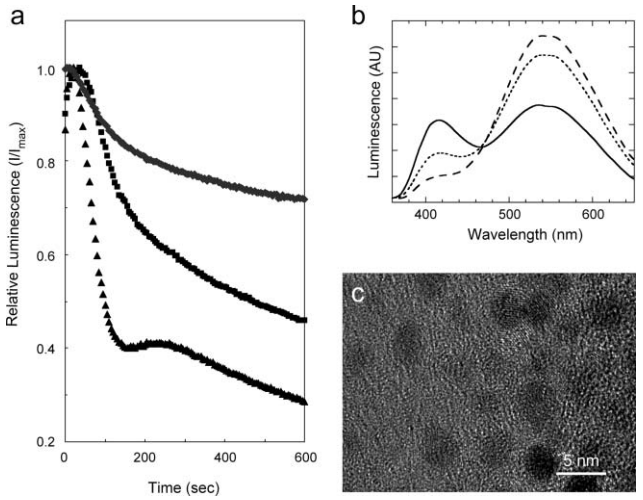

Fig. 2 (a) Kinetic luminescence measurements of an aqueous NH_2–ZnO nanocrystal solution (0.03 mg mL^{-1}) (♦) in the absence of *o*-phthalaldehyde (OPA), and in the presence of (■) 0.05 mM and (▲) 0.5 mM of OPA. The excitation and emission wavelengths were 345 nm and 545 nm, respectively. (b) Emission spectra of the aqueous NH_2–ZnO nanocrystal solution in the presence of OPA solutions of (- - -) 0.05 mM, (···) 0.125 mM and (—) 0.25 mM after being subjected to the kinetic luminescence experimental condition described in (a). (c) TEM images of the NH_2–ZnO nanocrystals after the kinetic luminescence experiment in the presence of 0.5 mM of OPA.

species from the –Si–CH_2–CH_2–CH_2– linker chain.[10] The signal broadening observed was consistent with the fact that the linker was in close proximity of the metal centers.

ZnO nanocrystals with mixed functional groups could also be synthesized using this strategy. Controlling the molar ratio between the aminoethylamino- and phosphonate-functionalized silanes in the reaction mixture allowed nanocrystals that have different surface charge and isoelectric points to be synthesized (see Fig. 1(c)). For example, at neutral pH, the ZnO nanocrystals functionalized only with aminoethylamine displayed positively charged colloidal properties: they were soluble in water and buffer solution. When the pH was increased to 10, the surface charge was reduced, and the nanocrystals would precipitate. By this strategy, soluble and variable pH stabilized ZnO nanocrystals could be achieved. It was found that aminoethylamine functionalization gave rise to ZnO nanocrystals with the best stability and the least polysiloxane side-products. This was possibly due to the strong affinity between the extended amino group and the ZnO surface, providing extra protection for the ZnO nanocrystals.

The luminescence intensity from nanoscale-confined crystals displayed a high dependency on the surfactant/protection layer surrounding these nanocrystals.[1a] Without proper protection layer, the luminescence intensity of nanocrystals would be reduced with light absorption. This photoleaching phenomenon was due to lattice distortion or crystal dissolution. If the protection layer was designed to interact with the desired chemical or biological targets, its characteristics and morphology could be altered upon binding. As a result, the luminescent nanocrystals would become more susceptible to photobleaching, and greatly reduced luminescence intensity would be observed upon light exposure. To prove this hypothesis, we applied ZnO nanocrystals protected by *N*-(2-aminoethyl)aminopropyltrimethoxysilane (AEAPS) (abbreviated as NH_2–ZnO nanocrystals), whose surface amine groups would react with aldehydes reversibly to form imines. This switching of the ZnO surface property would lead to luminescence quenching upon UV exposure. By fluorescamine titration, the amine concentration of our ZnO solution (3 mg mL^{-1}) was estimated at 2.2 mM.[6c] After diluted NH_2–ZnO nanocrystal solution (0.03 mg mL^{-1}) was continuously excited at a wavelength of 345 nm, a 29% reduction from the maximum luminescence intensity (545 nm) was observed after 10 min of exposure (see Fig. 2(a)). The luminescence intensity decreased further upon extended exposure. In the presence of 0.05 mM of *o*-phthalaldehyde (OPA), the surface amine groups of NH_2–ZnO nanocrystals would react reversibly with OPA to form imines. This gave rise to a greater reduction of 54% from the maximum luminescence after 10 min of UV exposure. We observed greater reduction in peak intensity at 545 nm with increasing OPA concentration. 71% luminescence quenching was obtained at 0.5 mM of OPA. It was also observed that a new emission peak at 419 nm emerged from the phenylimine luminophore (Fig. 2(b)). This new peak increased in intensity with increasing OPA concentration. This peak was from imine formation because control experiment between 2-amine-ethylamineethanol and OPA also gave rise to this peak.

TEM images show that the NH_2–ZnO nanocrystals were reduced from 5 nm to less than 4 nm after 10 min of UV exposure in the presence of OPA (Fig. 2(c)). This suggested that the reduced luminescence intensity resulted from increased photodissolution of ZnO nanocrystals after their surface amine groups reacted with OPA. The decreased photostability could be explained by the lower affinity between the imine groups and ZnO nanocrystals, compared to that between the amine groups and ZnO nanocrystals, leading to a more porous shell. Therefore, the core ZnO nanocrystals were more susceptible to photodissolution.

In order to diversely apply this methodology for selective detection, we employed a similar protocol as previously described for high-throughput screening.[11] This approach provided an easy access to a large volume of statistically meaningful data.

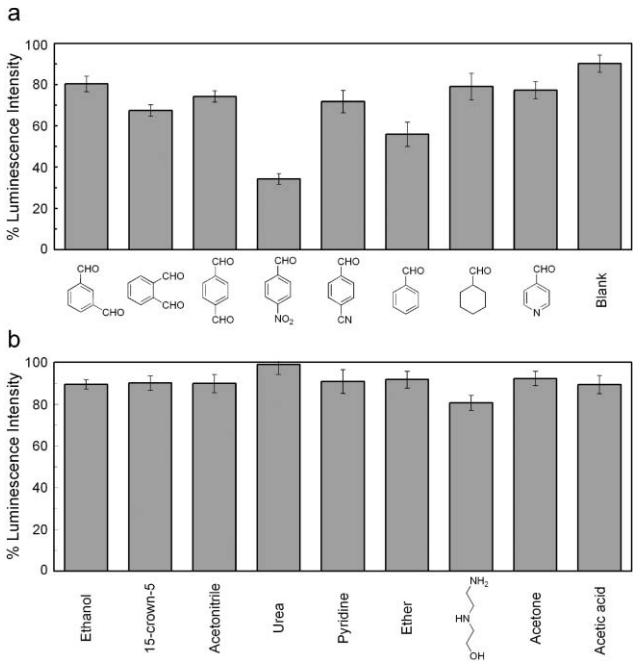

Fig. 3 Luminescence response of NH_2–ZnO nanocrystal solution (5 μg mL^{-1}) to 0.9 mM of various (a) aldehydes and (b) control compounds after 2 min of UV exposure.

Employing a 96-well microplate format, aldehyde and control compounds (0.9 mM) were dissolved in dimethyl sulfoxide (DMSO) due to their limited solubility in water. After synchronized mixing with an equal volume of aqueous NH_2–ZnO nanocrystal solution (5 μg mL^{-1}), the microplate was exposed to UV light from a flat-panel UV transilluminator (λ_{max} = 365 nm). The luminescence intensity at 545 nm (excited at 345 nm) was then recorded from a plate reader after 2 min of UV exposure. This set-up enabled us to develop the protocols of detection with high efficiency, and monitor the capability of the proposed detection method directly.

As shown in Fig. 3(a), the presence of various aldehydes (0.9 mM) generally quenched the luminescence of NH_2–ZnO nanocrystals by 20–70%, whereas only 10% of quenching was noted in the control after 2 min of UV exposure. It is noteworthy that even the aliphatic aldehydes responded similarly to the aromatic aldehydes under the protocol devised. The sensitivity and selectivity of this methodology allow for the detection of aldehydes related to physiological conditions, such as glucose for diabetes and acetaldehyde for driving under influence (DUI). Maximum luminescence intensity decay was 66% in the presence of *p*-nitrobenzaldehyde. The quenching effect of luminescence was not as significant as the earlier kinetic experiments. This was partly due to the much lower absorption coefficient of NH_2–ZnO nanocrystals at the wavelength of 365 nm, and partly due to the reduced UV exposure time. However, this protocol increased the efficiency of detection, and reproducible data were consistently obtained. Control experiments of photostability with organic compounds containing different functional groups all showed only minor reduction in luminescence intensity (Fig. 3(b)). The imine formation was highly favored with aldehyde groups. In contrast, organic compounds bearing similar carbonyl and carboxylic acid moieties (*e.g.* acetone and acetic acid) did not induce photostability switch. Only 2-amine-ethylamineethanol resulted in ~10% more intensity reduction amongst the control compounds.

In conclusion, we have applied a two-step surface functionalization approach using silane compounds to synthesize ZnO nanocrystals that possess increased colloidal stability and water solubility. Through this method, we have decorated ZnO nanocrystals with a variety of surface functional groups, and even with mixed functional groups. We have also demonstrated the first example of applying controlled photostability as a detection tool using the functionalized ZnO nanocrystals. A 29% reduction in the luminescence intensity occurred when the NH_2–ZnO nanocrystal solution was excited continuously at a wavelength of 345 nm. After reactions with aldehydes, the photostability of this system decreased, leading to a much greater reduction in luminescence intensity (by 71% for OPA). From control experiments, it was confirmed that the NH_2–ZnO nanocrystals behaved as selective agents for the detection of aldehydes. Expanding this methodology may pave the way for other biological/environmental sensing applications.

The authors thank Dr Yu Han and Dr Lan Zhao for their assistance with TEM. This work was funded by the Institute of Bioengineering and Nanotechnology (Biomedical Research Council, Agency for Science, Technology and Research, Singapore).

Notes and references

1 (*a*) X. Michalet, F. F. Pinaud, L. A. Bentolila, J. M. Tsay, S. Doose, J. J. Li, G. Sundaresan, A. M. Wu, S. S. Gambhir and S. Weiss, *Science*, 2005, **307**, 538; (*b*) P. Alivisatos, *Nat. Biotechnol.*, 2004, **22**, 47; (*c*) S. Kim, Y. T. Lim, E. G. Soltesz, A. M. De Grand, J. Lee, A. Nakayama, J. A. Parker, T. Mihaljevic, R. G. Laurence, D. M. Dor, L. H. Cohn, M. G. Bawendi and J. V. Frangioni, *Nat. Biotechnol.*, 2004, **22**, 93; (*d*) W. C. W. Chan, D. J. Maxwell, X. Gao, R. E. Bailey, M. Han and S. Nie, *Curr. Opin. Biotechnol.*, 2002, **13**, 40.

2 (*a*) A. P. Alivisatos, *Science*, 1996, **271**, 933; (*b*) C. B. Murray, D. J. Norris and M. G. Bawendi, *J. Am. Chem. Soc.*, 1993, **115**, 8706; (*c*) Z. A. Peng and X. Peng, *J. Am. Chem. Soc.*, 2001, **123**, 183.

3 (*a*) D. C. Look, *Mater. Sci. Eng., B*, 2001, **80**, 383; (*b*) S. Cho, J. Ma, Y. Kim, Y. Sun, G. K. L. Wong and J. B. Ketterson, *Appl. Phys. Lett.*, 1999, **75**, 2761; (*c*) T. K. Gupta, *J. Am. Ceram. Soc.*, 1990, **73**, 1817; (*d*) M. J. Brett and R. R. Parsons, *Solid State Commun.*, 1985, **54**, 603.

4 (*a*) E. A. Meulenkamp, *J. Phys. Chem. B*, 1998, **102**, 5566; (*b*) N. S. Norberg and D. R. Gamelin, *J. Phys. Chem. B*, 2005, **109**, 20810; (*c*) M. Monge, M. L. Kahn, A. Maisonnat and B. Chaudret, *Angew. Chem., Int. Ed.*, 2003, **42**, 5321; (*d*) H.-M. Xiong, D.-P. Liu, Y.-Y. Xia and J.-S. Chen, *Chem. Mater.*, 2005, **17**, 3062; (*e*) H.-M. Xiong, Z.-D. Wang, D.-P. Liu, J.-S. Chen, Y.-G. Wang and Y.-Y. Xia, *Adv. Funct. Mater.*, 2005, **15**, 1751.

5 (*a*) S. T. Selvan, T. T. Tan and J. Y. Ying, *Adv. Mater.*, 2005, **17**, 1620; (*b*) N. Gaponik, D. V. Talapin, A. L. Rogach, K. Hoppe, E. V. Shevchenko, A. Kornowski, A. Eychmuller and H. Weller, *J. Phys. Chem. B*, 2002, **106**, 7177.

6 (*a*) D. Gerion, F. Pinaud, S. C. Williams, W. J. Parak, D. Zanchet, S. Weiss and A. P. Alivisatos, *J. Phys. Chem. B*, 2001, **105**, 8861; (*b*) W. J. Parak, D. Gerion, D. Zanchet, A. S. Woerz, T. Pellegrino, C. Micheel, S. C. Williams, M. Seitz, R. E. Bruehl, Z. Bryant, C. Bustamante, C. R. Bertozzi and A. P. Alivisatos, *Chem. Mater.*, 2002, **14**, 2113; (*c*) A. Schroedter and H. Weller, *Angew. Chem., Int. Ed.*, 2002, **41**, 3218; (*d*) A. Schroedter, H. Weller, R. Eritja, W. E. Ford and J. M. Wessels, *Nano Lett.*, 2002, **2**, 1363.

7 N. R. Jana, Y. Chen and X. Peng, *Chem. Mater.*, 2004, **16**, 3931.

8 H. Zhou, H. Alves, D. M. Hofmann, W. Kriegseis, B. K. Meyer, G. Kaczmarczyk and A. Hoffmann, *Appl. Phys. Lett.*, 2002, **80**, 210.

9 (*a*) D. W. Bahnemann, C. Kormann and M. R. Hoffmann, *J. Phys. Chem.*, 1987, **91**, 3789; (*b*) A. V. Emeline, V. K. Ryabchuk and N. Serpone, *J. Phys. Chem. B*, 1999, **103**, 1316.

10 See Electronic Supplementary Information.

11 J. N. Cawse, *Acc. Chem. Res.*, 2001, **34**, 213.

